Effects of Processing Parameters in P/M Steel Forging on Part Properties: A Review

Part III Analysis Methods

R. Duggirala and R. Shivpuri

In the last decade, powder metallurgy (P/M) technology has made marked advances in competitive manufacturing. P/M offers design opportunities that are not possible with other methods, as well as significant cost savings. The processing parameters, material characteristics, individual stages of parts production, deformation and densification mechanics and tooling, and preform design influence the properties of the P/M part and related economics. Therefore, a review of the various parameters involved in the different stages of P/M steel forging in net-shape manufacturing and their implications on resulting properties of P/M parts is presented in a three-part review. Part I discusses the stages of preparing a sintered compact, and Part II identifies key parameters in forging the sintered compact that influence the properties of the powder forged part. Part III reviews the different analysis methods available to study P/M processing.

1. Introduction

FORGING of powder metal preforms is currently of considerable interest due to the increase in such applications. To effectively forge P/M parts, it is necessary to control several contributing parameters to ensure uniform densification, avoidance of cracking, elimination of flash formation, and the required mechanical properties. This is achieved by detailed consideration of die design, preform design and lubrication, and in-depth understanding of the deformation mechanics during the forging of P/M materials. The porosity of sintered P/M parts that are forged causes the behavior of sintered parts to deviate from those of conventional cast and wrought materials. In the following sections, plasticity theories proposed for porous materials based on classical methods, numerical approaches in P/M forging, and analysis methods for die design in P/M forging are presented.

There are numerous combinations of powder metallurgy and deformation processing and some of the key combinations are listed in Table 1. However, in this review, the focus is on powder forging. The process of powder forging and the influence of different parameters during processing on the mechanical properties of the forged part have been reviewed in Parts I and II in this issue.

R. Duggirala is the Senior Project Engineer at the Saginaw Division of General Motors, and **R. Shivpuri** is Assistant Professor in Industrial and Systems Engineering at Ohio State University.

2. Plasticity Theory and Yield Criterion for Porous Materials

In the case of fully dense materials, constancy of volume during plastic deformation is maintained, and the value of the plastic Poisson ratio equals 0.5. The effect of hydrostatic stress in yielding is negligible, if not absent. Porous materials, how-

Table 1 Processes Combining P/M with Deformation Operations[1]

Process	Material	Ref
Near-net-shape products		
Compaction of preform—sintering—precision forging	Net-shape steel part	3,4
Compaction of preform—sintering—(cold) forging	Near-Net-shape part (steel, aluminum alloys)	5,6
Compaction of preform—sintering—gear rolling—machining	Helical gears from sintered steel	7
Can-hot isostatic pressing of preform—Decan—hot forge—machining	Near-net-shape part (Superalloys,Titanium)	8
Semifinished products		
Can—hot isostatic pressing—hot work	High speed steel	9
	Stainless steel	10
Cold isostatic pressing—vacuum sintering—hot work	High speed steel	11
Controlled spray deposition—hot work	Stainless steel	12
	Low-alloyed steel	13
Compaction by rolling—sintering—hot rolling—cold rolling	Nickel-base alloys	14
Can—vacuum degas—hot press—decan—hot work	Aluminum alloys	15,16
Cold isostatic pressing—vacuum degas—extrude	Aluminum alloys,metal matrix composites	17,18
Vacuum hot pressing—extrude	Aluminum alloys	19
Continuous forming	Aluminum-copper alloys	20

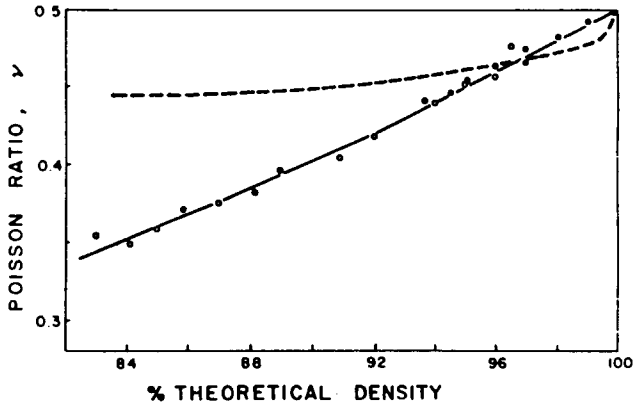

Fig. 1 Comparison of predicted ν versus ρ relationship due to Green[4] with experimental relationship.

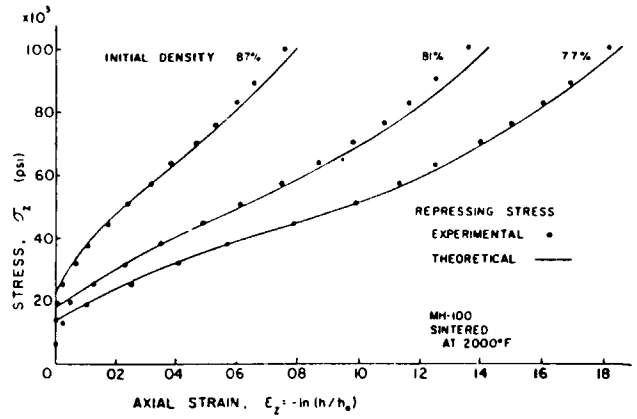

Fig. 2 Comparison of theoretical and experimental results for axial stress in repressing iron powder compacts.[5]

ever, differ in that there is a change in volume during plastic deformation, and the hydrostatic stress component influences yielding. Yield behavior of other materials sensitive to the hydrostatic stress has been studied previously[2,3] for yielding of soil and loose powder compaction often referred to as granular media.

A plasticity theory was proposed by Green[4] for P/M materials that considers a solid weakened by numerous cracks or voids. The assumptions made in this theory were that the material is isotropic, rigid-perfectly plastic, void growth or decay occurs isotropically, and that the cavities are more or less spherical in shape. The above assumptions are reasonable for deformations that are not too severe, and when elastic effects are ignored. This results in a yield surface of the form:

$$J_2' + \alpha J_1^2 = \delta Y^2$$

where J_1 and J_2' are invariants, α and δ are functions of v, the void ratio (volume of voids to volume of solid plus voids). The amount by which the yield stress is lowered due to the presence of spherical voids in an otherwise solid material was quantitatively predicted, and the method of determining yield stress of

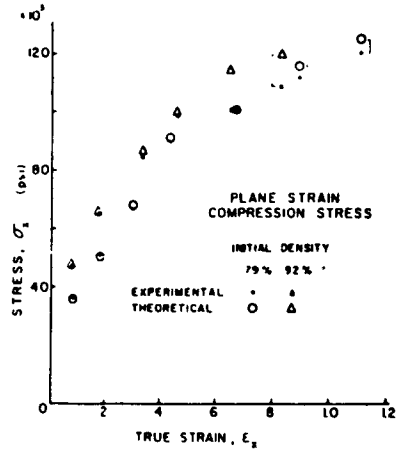

Fig. 3 Comparison of theoretical and experimental stress in plane-strain compression of sponge iron powder.[5]

the porous material is described including yielding due to mean pressure. A constitutive law of the hypoelastic type was derived. The Poisson's ratio for porous materials is shown as a function of instantaneous density in Fig. 1. This approach, however, overestimates the experimental measurements of Poisson ratio at low densities and predicts lower sensitivity to increasing density.

Stress-strain curves in uniaxial compaction of iron powder were determined and Poisson's ratio was evaluated by Kuhn and Downey.[5] These results formed the basis for their proposed plasticity theory. In the development of the theoretical mechanics of plastic deformation of any material, a criterion of yielding and a flow rule between stress and strain needs to be established. For a sintered P/M material, hydrostatic stress does cause yielding, and therefore, the yield criterion must be a function of hydrostatic and deviatoric stress and it must reflect the influence of increasing density. These results must reduce to that for a conventional material as full density is approached. The proposed yield criterion satisfying the above requirements is

$$f = [3J_2' - (1 - 2\nu)J_2]^{1/2}$$

where J_2' is the stress deviator, J_2 is the second invariant of stress, ν is the Poisson's ratio, and f is the magnitude of yield stress of the material in simple compression. Because cold working and densification in P/M are not independent, $f = Y(d)$, where d represents density. The stress-strain relation was expressed using the normality flow rule proposed by St. Venant where the plastic strain increment is normal to the yield surface.

Using the above theory, experiments of axisymmetric repressing were conducted and compared with the theoretical values, as shown in Fig. 2. The results were found to be in good agreement except at high stresses, which is attributed to errors in experimental procedures in terms of sintering, shrinkage, etc. Comparison of theoretical and experimental stresses in plane-strain compression of sponge iron powder (Poisson's ratio versus density data were available for this material) is shown in Fig. 3 which shows good correlation except for high

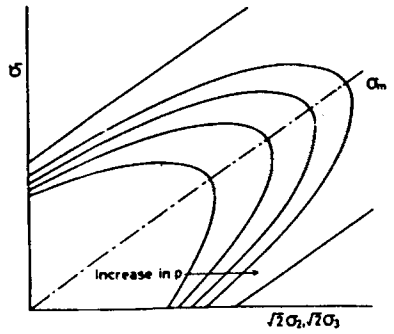

Fig. 4 Schematic illustration of yield surfaces for porous materials.[6]

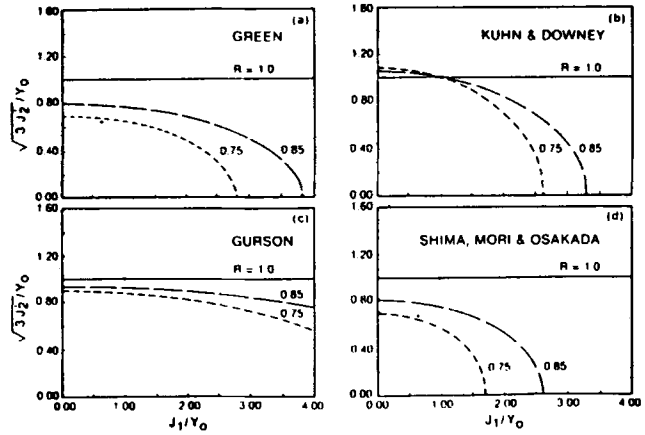

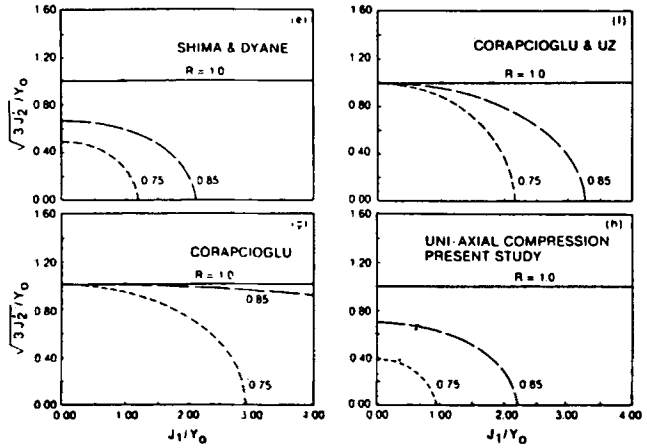

Fig. 5 Yield functions proposed by various researchers.[7]

stresses. The work hardening coefficient for a P/M material is found to be an inverse function of sintered density of compacts, and work hardening was due to densification and cold working of material surrounding the pores as opposed to mobility of dislocations in conventional material.

In the above two theories proposed for porous metals, the yield criterion is a function of the first invariant of stress and second invariant of deviatoric stress, and the stress-strain relations are of the form:

$$d\varepsilon_i = d\lambda(\sigma_i - \varphi\sigma_m)(i = 1,2,3)$$

where $d\lambda$ is a non-negative constant that is not evaluated. Therefore, these approaches are used only for simple stress states such as uniaxial compression and tension or plane-strain compression and are not satisfactory for the analysis of practical deformation processes.

Shima and Oyane[6] derived basic equations of plasticity for porous materials similar to the ones just discussed and applied the theory to applications such as frictionless closed die compression. The yield criterion for sintered materials

$$f = \left[\{ (\sigma_1 - \sigma_2)^2 + (\sigma_2 - \sigma_3)^2 + (\sigma_3 - \sigma_1)^2 \} / 2 + (\sigma_m / f)^2 \right]^{1/2}$$

is used where f represents the degree of influence of the hydrostatic component s_m. A function f' is introduced where f' represents the ratio of apparent stress applied to the porous bodies and the effective stress applied to the matrix and maybe a function of relative density. A schematic illustration of the yield surfaces for porous materials is shown in Fig. 4. Simple tension and compression tests of sintered copper were carried out to enable determination of f,n, and f'. These two functions (f and f') were found applicable to sintered iron and aluminum, whereas the equations derived for copper were found to be applicable to the results of Kuhn *et al.*[5] by representing:

$$\nu = 0.5(1 - \tfrac{2}{9}f^2) / (1 + \tfrac{1}{9}f^2)$$

Yield functions proposed by various researchers are shown in Fig. 5 and Table 2. The large differences between the various theories emphasize the need for a yield function for porous materials that is derived from a physically based criterion. It is to this effort that Doraivelu *et al.*[7] proposed a new yield function for compressible P/M materials based on a yield criterion also postulated by the above authors. The yield criterion for porous bodies proposed that "homogeneous and isotropic porous materials begin to yield when the apparent total deformation energy, considering porous materials as continuous, reaches a critical value." The behavior of porous materials is assumed to be linear up to the yield point with no permanent change in density, and densification begins only after yielding. The representation of yield function in terms of principal stresses is given as:

$$\sigma_1^2 + \sigma_2^2 + \sigma_3^2 - R^2(\sigma_1\sigma_2 + \sigma_2\sigma_3 + \sigma_3\sigma_1) = (2R^2 - 1)Y_o^2$$

R being relative density and Y_o the yield stress for fully dense material. This representation shows growth of yield surface with densification and eventually becomes independent of the hydrostatic stress (J_1) at fully density. The experiments were conducted on aluminum alloy X7091, and the function pro-

Table 2 Yield Functions Proposed by Other Researchers

Reference	A, B, and δ as a function of R	$3(1-B)$	Remarks
Green[1]	$A = 3$ $B = \frac{1}{4[\ln(1-R)]^2}$ $\delta = \frac{3[1-(1-R)^{1/3}]^2}{3-2(1-R)^{1/4}}$	$3-\left[\frac{3}{4[\ln(1-R)]^2}\right]$	When $R = 1$, $B = 0$ and $\delta =$ When $R = 0$, $\delta = 0$, and $B \rightarrow \infty$
Gurson[2]	$A = 3$ $B = \frac{(1-R)^2}{8}$ $\delta = (R^2 = R+1)$	$3 - [3/8(1-R^2)]$	When $R = 1$, $B = 0$ and $\delta = 1$ When $R = 0, \delta = 1$, δ never reduces to zero
Kuhn and Downey[3]	$A = 2 + R^2$ $B = \frac{(1-R^2)}{3}$	$2 + R^2$	$A = 3(1-B)$ $\delta = 1$ at density levels When $R = 1, B = 0$
Oyane *et al.*[4]	$A = 3/R^2$ $B = \frac{1}{[1+\sqrt{R}/(1-R)]^2 R^2}$ $\delta = R^2$	$3-\left\{\frac{3}{[1+\sqrt{R}/(1-R)^2 R^2}\right\}$	When $R = 1$, $B = 0, \delta = 1$ When $B = 0$, $\delta = 0$ and $B \rightarrow \infty$
Shima and Oyane[5,6]	$A = 3$ $B = \frac{2.49(1-R)^{0.514}}{9R^5}$ $\delta = R^5$	$3-\left[\frac{7.47(1-R)^{0.514}}{9R^5}\right]$	When $R = 1$, $B = 0$ and $R = 0$ When $R = 0, \delta = 0$, and $B = \rightarrow \infty$
Shima *et al.* [5,6] (Refer to Appendix A)	$A = 3/(1+\mu)$ $B + \frac{\mu}{1+\mu}$ $\delta = \frac{R^2}{1+\mu}$	$3/(1+\mu)$	When $R = 1$, $\mu = 0, A = 3$, $B = 0$, and $\delta = 1$
Corapcioglu[7]	$A = 3$ $B = 2.091(1-R)^2/R^2 - \frac{0.26(1-R)}{R^2}$ $\delta = 1$	$3 - 6.27(1-R^2)/R^2 - \frac{0.78(1-R)}{R^2}$	$\delta = 1$ at all density levels When $R = 1$, $B = 0$ When $R = 0, B \rightarrow \infty$
Corapcioglu and Uz[7]	$A = 3$ $B = \frac{0.361(1-R^2) + 0.39(1-R)}{R^2}$ $\delta = 1$	$3 - \frac{1.083(1-R^2)}{R^2} + \frac{1.2(1-R)}{R}$	$\delta = 1$ at density levels When $R = 1$, $B = 0$ When $R = 0$ $B \rightarrow \infty$

From Ref. 7.

posed was verified for the density dependence of the yield and geometrical hardening.

3. Friction in Powder Forging

Friction between the preform and die surfaces during forging plays a major role in determining the process characteristics. Reducing friction decreases tonnages required for forging, facilitates easy ejection of the forged part, and improves tool life. It also enables forming of parts with thin and long sections, improves surface finish, and prevents cracking and fracture of the part during forging.

Typical representations of friction in metalworking applications are coulomb (friction is directly related to the pressure normal to the sliding surfaces), shear (friction force is related to the workpiece shear yield strength), and in recent developments as a function of relative velocity between the two surfaces.[8] The ring test has been used for evaluating friction in forging of fully dense materials and can also be applied to powder forging.[9] Calibration curves (Fig. 6) are generated from ring tests[8] for different friction factors, and densities are determined from changes in the dimensions of the rings in the test. This figure can then be used to provide a quantitative comparison of friction for various lubricants, die materials, surface finishes, temperature effects, etc.

4. Fracture Mechanisms and Forming Limits in Forging of Sintered Preforms

Fracture during plastic deformation of fully dense materials that are ductile initiates by void formation at inclusions or other inhomogeneities in the metal matrix. The pre-existence of voids in material such as in P/M materials, eliminates the need for void initiation, and only coalescence of voids is necessary for crack formation.

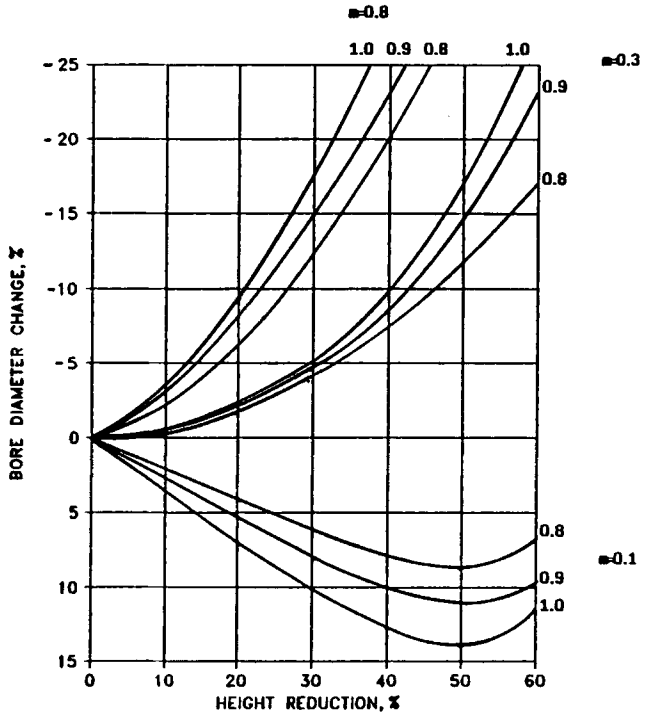

Fig. 6 Calibration chart for ring tests on sintered powder material. Relative density values are 1.0, 0.9, and 0.8. Note that for each friction value the change in bore diameter decreases with decreasing density (ring proportions OD:ID:H = 6:3:2).[8]

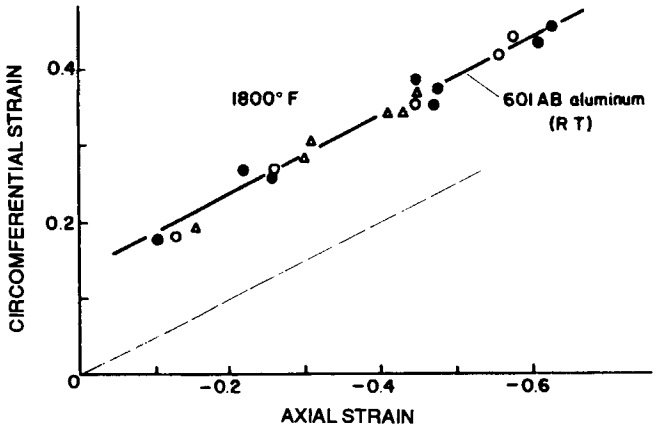

Fig. 7 Locus of surface strains at fracture during upsetting of sintered 4620 low-alloy steel powder cylinders. Induction sinter: ● 2350 °F for 3 min, ○ 2050 °F for 3 min. Δ Conventional sinters; 2050 °F 1/2 hr.[10]

A locus of surface strains at fracture (forming limit diagram) during upsetting of 4620 steel alloy (Fig. 7) is determined by measuring the axial and circumferential strain of the bulge surface (Fig. 8). This locus is used as fracture criterion for the evaluation of the deformation to fracture in more complex de-

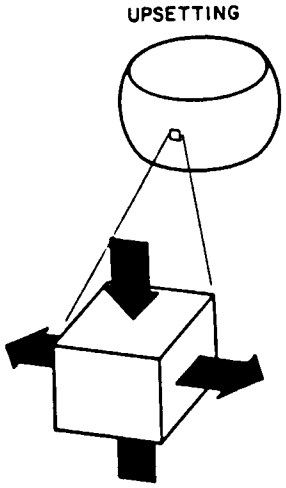

Fig. 8 Circumferential tensile stress and axial compressive stress at the bulge surface of cylinders compressed axially with high contact friction.[10]

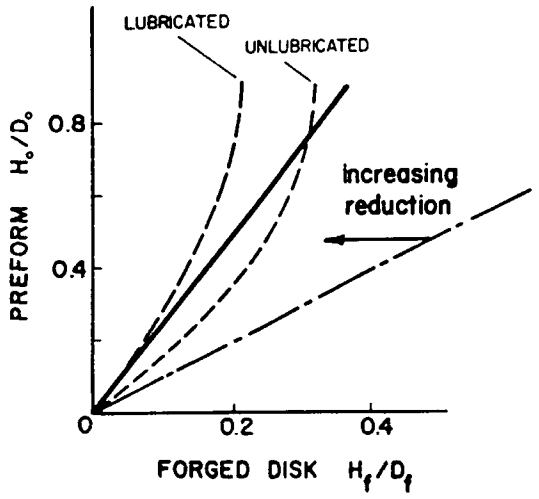

Fig. 9 Design curves for disk forging to achieve maximum mechanical properties (left of solid line) without causing fracture during forming (right of dashed line).[10]

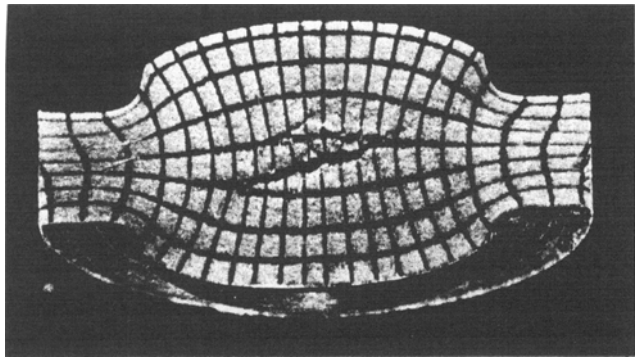

Fig. 10 Central burst in a forged part consisting of two opposed hubs. Grid lines placed on midplane prior to deformation to permit measurement of internal strains.[10]

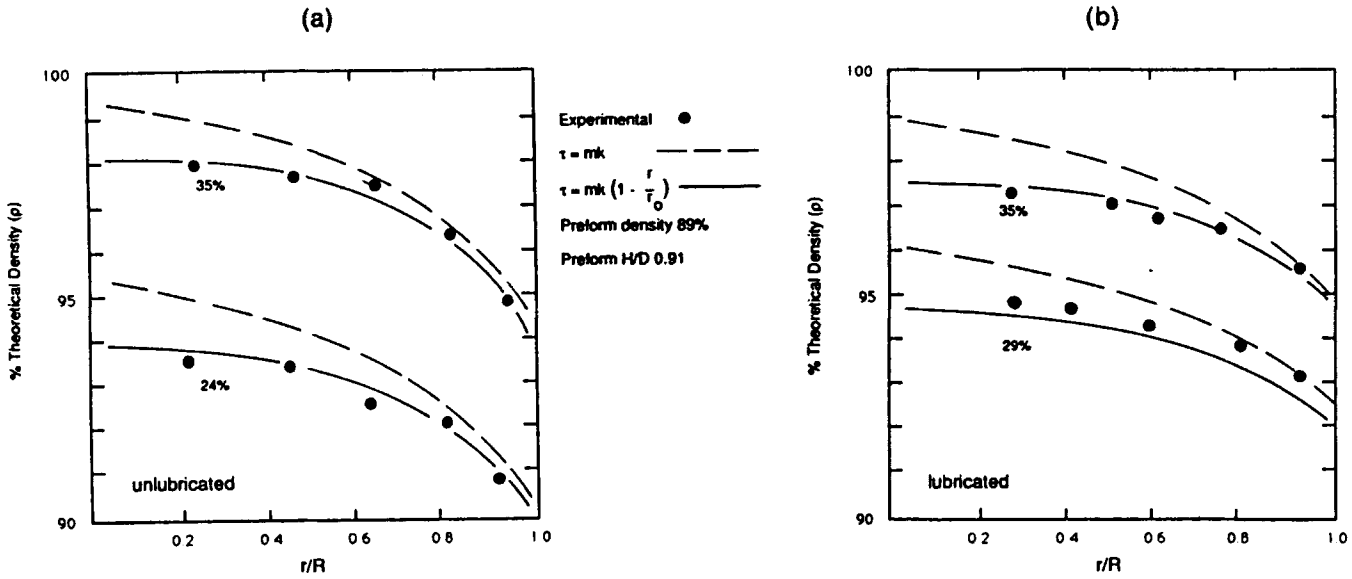

Fig. 11 Radial distribution of density during compression of sintered powdered aluminum. (**a**) Unlubricated. (**b**) Lubricated with MoS_2 in grease. Solid lines show calculated results for velocity-dependent shear, whereas the dashed lines show results for constant shear friction model.[8]

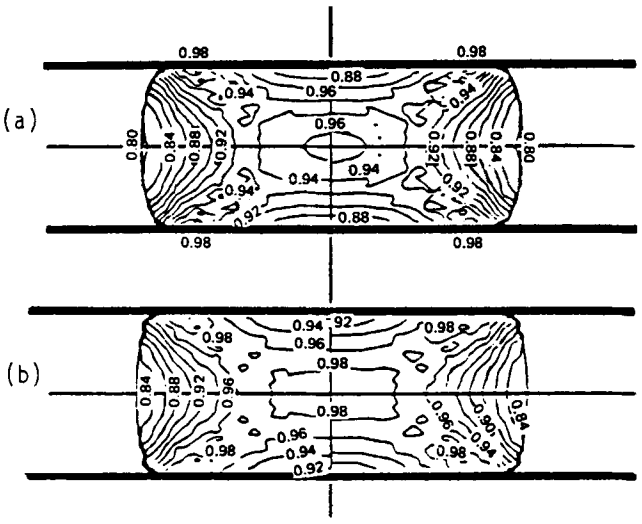

Fig. 12 Relative density distributions at 40% reduction in height with two friction conditions: left ($m = 0.5$), right ($m = 1$). (**a**) Case 1 ($Ro = 0.743$). (**b**) Case 2 ($Ro = 0.802$).[20]

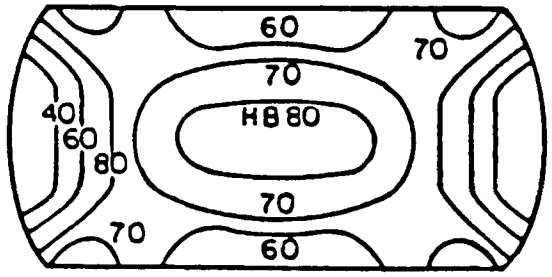

Fig. 13 Experimental local hardness distribution in the center cross section of a bar.[20]

formation processes. The progressing deformation strain paths in the potential fracture regions of the process under consideration are first determined through plastic analysis or measurements on a model material. These strain paths are then compared with the fracture locus of the material. If the strain paths cross the fracture locus before the deformation process is complete, fracture is likely. This locus of fracture strain is primarily for free surface fracture.

An example of methodology of preform design for a disk forging is presented. This provides for sufficient metal flow to achieve maximum density, but less than that at which fracture occurs. Given a disk diameter and a height, fracture in upsetting can be avoided if the expanding free surface of the cylinder reaches the die sidewalls before the reduction at fracture is reached. The preform's aspect ratio versus forged disk aspect ratio is plotted, as shown in Fig. 9. For a given preform aspect ratio, the forged disk aspect ratio must be to the left of the solid line to achieve maximum properties of 50% reduction, and the forged disk aspect ratio must be to the right of the dashed line to avoid fracture.

Evaluation of more complex shaped forgings and corresponding fracture criterion are presented in Ref. 8. Figure 10 shows internal fracture occurring in a part. Evaluation of internal strains enable possible prediction of such failures.

5. Plasticity and the Slab Method Approach

Kuhn and Downey (1973) have derived simple analysis methods based on the plasticity principles discussed earlier and

on the slab method approach to frictionless axisymmetric and plane-strain compression. Analytical approaches for simple forging such as compression, upsetting, and repressing are discussed in Chapter 4.III of Ref 10, which also includes the frictional effects at the die/workpiece interface, as shown in Fig. 11. Comparison of the analytical results from the slab method in compression with friction at the die surfaces showed good correlation with experimental measurements. Densities and pressures are determined using this method. The above analytical approaches are applicable for simple shapes, but for complex shapes numerical methods are more effective.

6. Thermal Analysis

In hot forging of P/M parts, transfer of heat from part to dies and the surrounding atmosphere occurs, as well as heat gain by part due to deformation. Localized chilling at die/workpiece contact areas produces poor properties in the forged part. Significant temperature gradients within the workpiece could result in residual stresses and distortion. Dimensional changes occur due to shrinkage and expansion. Therefore, analysis methods need to be applied to determine the above effects prior to forging. Several analytical tools exist for determining heat transfer, gain, and loss that occur during P/M forging by conduction, convection, and radiation. Some of the thermal processes are discussed in Ref 8.

7. Simulation of P/M Forging—Numerical Methods

In the area of modeling of metal forming processes, finite elements methods have been applied successfully. User-oriented rigid viscoplastics finite element method codes have further made these methods easier to use and more efficient. The applicability of these methods has been extended to the area of powder metal fabrication where the material model includes the behavior of porous metals.

Oyane *et al.* derived plasticity equations from the yield function proposed by Kuhn. Based on these equations, slip-line field solutions and upper-bound solutions applicable to porous metals were derived.[11-14] These researchers extended the above theory in developing the rigid plastic finite element method of analysis of metal forming.[14]

Im and Kobayashi[15] developed a formulation somewhat different, although based on the same principle as the above theories. The governing equations for the boundary value problem were derived for porous metals as:

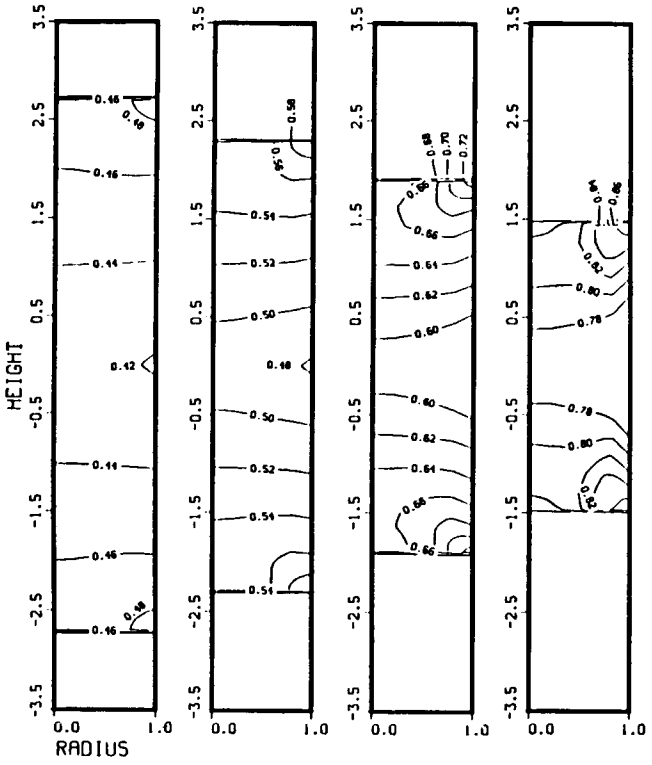

Fig. 14 Prediction of relative density distribution of solid cylinder at 12.9% (0.4478), 25.8% (0.5256), 38.7% (0.6363), and 51.6% (0.806) reductions in height (average compact density) with double-action press.[24]

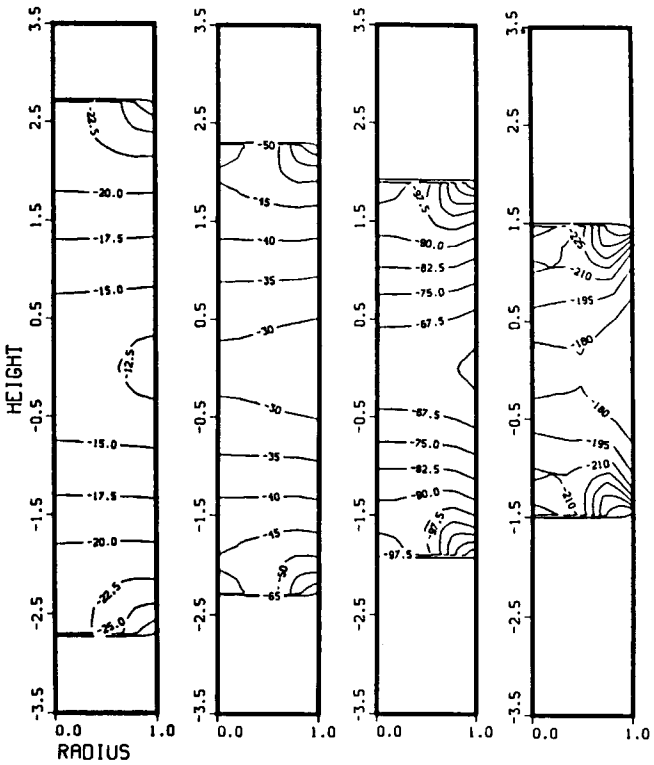

Fig. 15 Prediction of mean stress (MPa) distributions of solid cylinder at 12.9% (0.4478), 25.8% (0.5256), 38.7% (0.6363), and 51.6% (0.806) reductions in height (average compact density) with double-action press.[24]

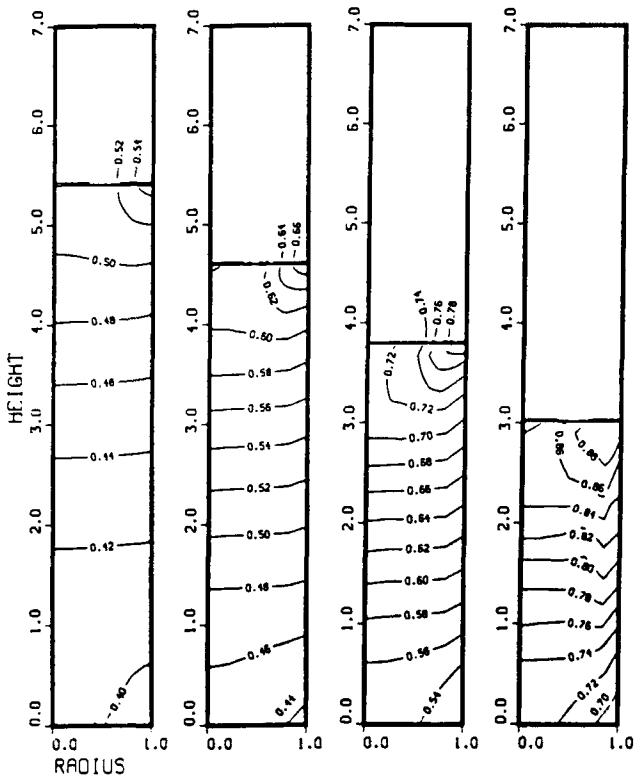

Fig. 16 Prediction of relative density distributions of solid cylinder at 12.9% (0.4478), 25.8% (0.5256), 38.7% (0.6363), and 51.6% (0.806) reductions in height (average compact density) with single-action press.[24]

Equilibrium conditions: $\sigma_{ij,j} = 0$

Compatibility: $\varepsilon_{ij} = 0.5(U_{i,j} + U_{j,i})$

Flow rules: $\varepsilon_{ij} = \delta F / \delta\sigma_{ij}\,\lambda$

σ_{ij} and ε_{ij} are apparent stresses and strain rates, respectively, considering porous metal as a continuum. Boundary conditions are next set up for the boundary surface, $S = S_t$ (traction) + S_u (velocity) + S_c (tool/workpiece interface) and n_j is the unit outward normal to surface. The yield function and flow rule are then defined where the effective strain-rate is defined according to Hill[16] and Johnson and Mellor.[17] The variational form of equilibrium equations used for discretization is derived.

The material properties are defined by the apparent yield stress, Y_r, and relative density R[7] discussed in an earlier section. The effects of strain, strain rate, and temperature on the yield stress are also included as $Y_b = Y_b(\varepsilon_b, \varepsilon_b, T_b)$, with b denoting the base metal.

Discretization is accomplished by using an isoparametric quadrilateral element with a bilinear distribution function, and stiffness equations are derived that are nonlinear. The Newton-Raphson method is used for solving nonlinear equations. The treatment of the rigid zone is based on the magnitude of the prevailing strain rate and expressing stress-strain rate relationships accordingly. Relative density is updated by relating volumetric strain rate to relative density. The function boundary

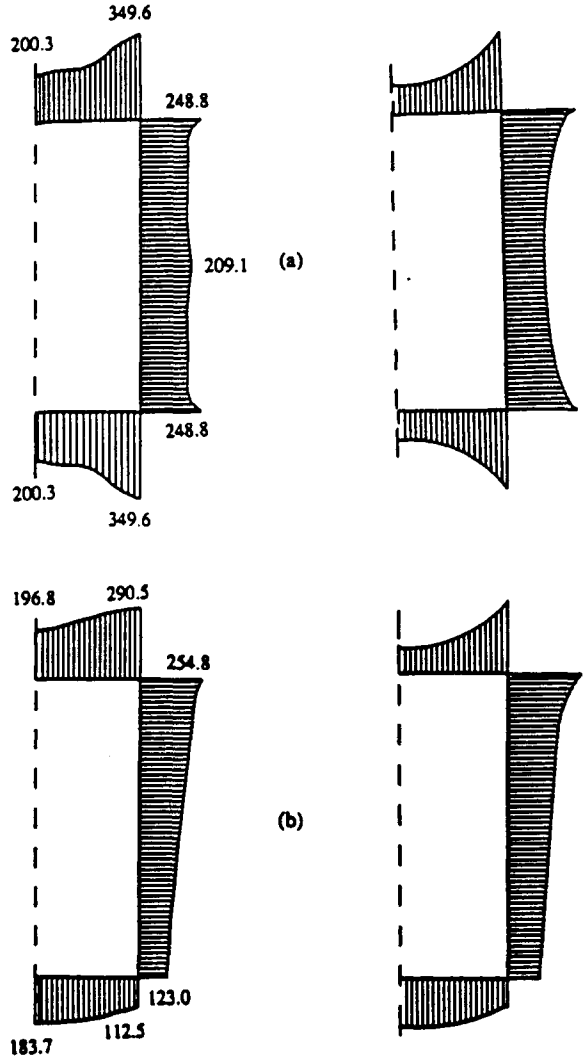

Fig. 17 Predicted pressure (MPa) distributions along die walls and punches of solid cylinder compacts (left) and schematic diagram of experimental observation[24] (right) for (**a**) double-action press and (**b**) single-action press.[24]

condition is represented by a velocity-dependent frictional stress, expressed as:

$$f = mk\left\{2/\pi\tan^{-1}[\,|Vdw|/a]\right\}$$

where k is shear strength, Vdw is the relative velocity of workpiece material with respect to die, a is a constant several orders of magnitude smaller than the die velocity, and m is the friction factor, varying from 0 to 1.

Applying the above principles and modifying existing computer software ALPID, to include compressibility of material, Oh[18] modified the code and tested by analyzing compression of cylindrical porous material. An element with relative density ($R = 0.999$) was considered fully dense to stabilize convergence of solution. Performing volume integration by Gaussian quadrature and using reduced integration for volumetric strain rate were found to be efficient.

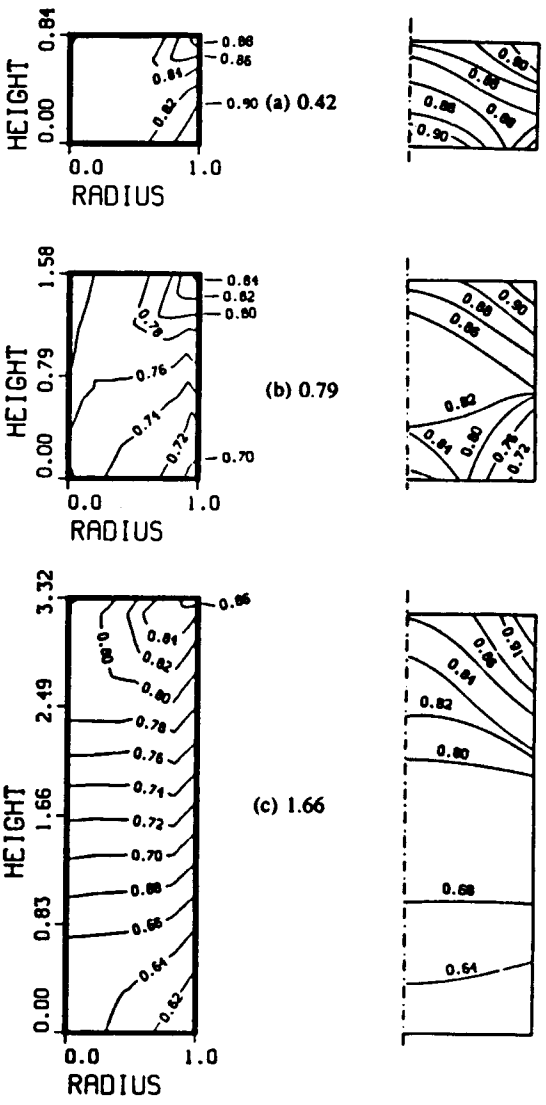

Fig. 18 Comparison between relative density distributions of simulations (left) and that of experiments[21] (right). Compact height to diameter ratios (initial H/*D* ratios of simulation) of (**a**) 0.42 (0.9), (**b**) 0.79 (1.6), and (**c**) 1.66 (3.1).[24]

Ring compression and axisymmetric forging were two example problems analyzed. In the above analysis, isothermal conditions were assumed. Figure 12 shows densification for two friction conditions, and Fig. 13 represents the experimental local hardness distribution for the same, which compares with the density distribution. Im and Kobayashi[19] developed a remeshing program based on the area-weighted-average technique and tested by simulating forging of the flange-hub shape. An analysis using this technique was performed for the forging of a pulley blank. The remeshing procedure may be subdivided into the following steps:

1. Generating a new mesh system
2. Determining the values (apparent strains and relative densities) of the nodal points in old mesh

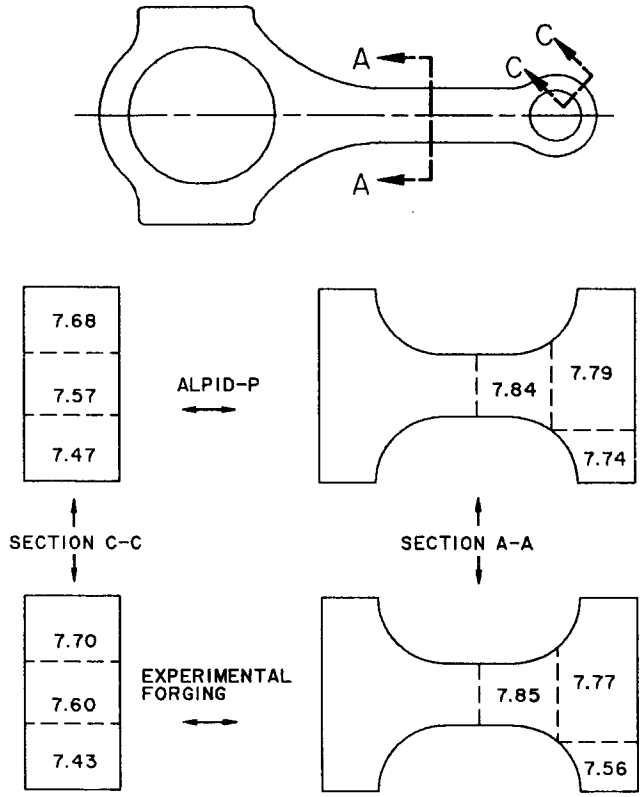

Fig. 19 Comparison of ALPID-P versus experimental bulk density (g/cm^3) estimated at sections A-A and C-C.[30]

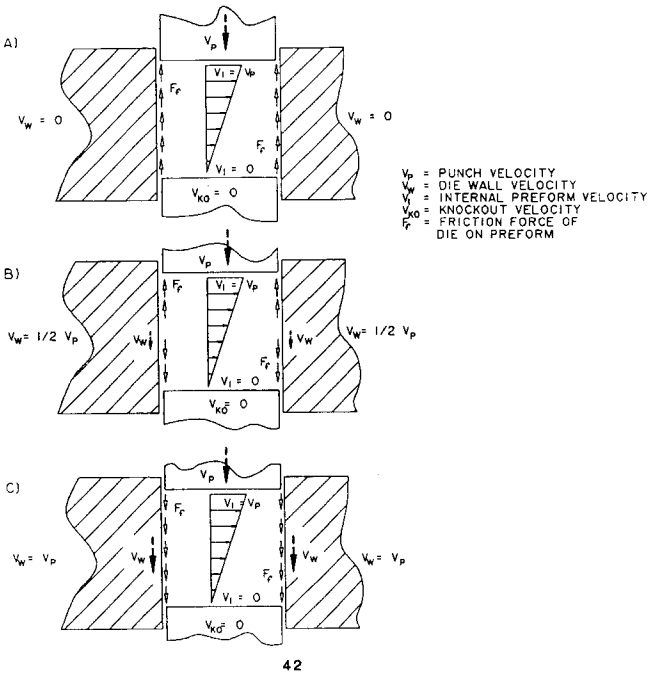

Fig. 20 Effect of die wall velocity on interface friction.[30]

3. Determining the values (nodal velocities, apparent strains, and relative densities) of the nodal points in the new mesh system by interpolation

4. Determining apparent strain and relative densities at the center of each new element, checking the boundary condition, and generating the new element connectivity if the number of elements is changed.

The detailed deformation characteristics for the different preform shapes under two frictional conditions were obtained. It was demonstrated that the program could be used in preform design in P/M forging and that remeshing is an indispensable tool for simulating metal flow involving complex geometries and large deformations.

Im and Kobayashi[20] enhanced their formulation by accounting for the effect of temperature, and the modified program was applied to plane-strain compression of sintered iron powder bar. The formulation used a phenomenological approach for the deformation analysis, in which the yield stress is determined from the yield stress of the base material and the relative density of the workpiece, as described earlier. This is an extension to the coupled analysis of transient viscoplastic deformation and heat transfer by Rebelo and Kobayashi.[21] A simple linear relationship between thermal conductivities of the powdered material and the base metal was derived and used as a first approximation in temperature calculation. The coupled analysis of deformation and heat transfer determined the dimensional changes, densification, stress and strain, strain distributions, temperature distributions, and material flow during forging. It was found that the effect of friction is significant in the deformation analysis (fracture at free surface occurred for large friction rather than for small friction), but negligible for the temperature calculation. Good correlation of computation results to experiments confirmed the validity and capability of this program.

Oh and Gegel[18] and Oh *et al.* [22] have presented the implementation of the P/M constitutive equations proposed by Gegel *et al.*[7] as discussed earlier, into the general purpose finite element method code ALPID to simulate P/M forming processes. A variational functional of the rigid viscoplastic porous material was derived based on the above constitutive equations. Solutions determined using the formulation for simple compression and die pressing with different frictions were compared with experimental measurement and found to be in good agreement.

Hwang and Kobayashi developed a plasticity theory for a powdered metal compact.[23] The yield criterion used for sintered powder compacts was modified for describing the asymmetric behavior of green powder compacts in tension and com-

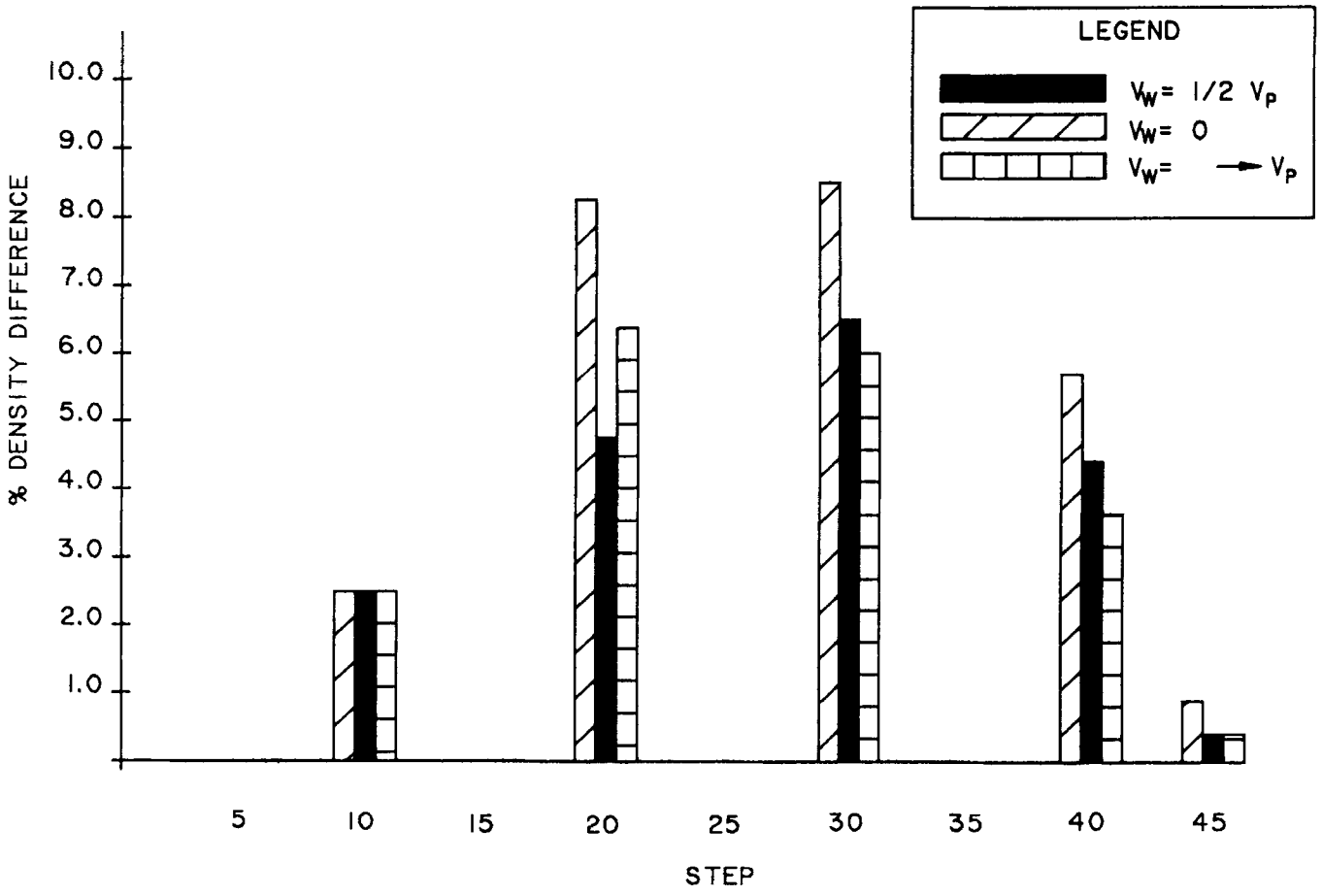

Fig. 21 Effect of die wall velocity on densification uniformity.[30]

pression and the finite element formulation derived.[24] An isoparametric quadrilateral element with a bilinear shape function is used for discretization. To handle regions of the body that become rigid without solution instability, a strain-rate offset is used at the rigid regions. The deformation is characterized by determining the parameters α, p, and apparent effective stress, σR as a function of relative density R. The parameters were determined from the behavior of sintered powder compacts and from the relationship between green strength and relative density for powder metal compacts.[23] σR is expressed in terms of R and Rc (critical density close to the tap density), the parameter α in terms of R, and p in terms of α, σR, and the green strength σt. Also, the coulomb friction law was used to represent friction, because it was found well suited for representing powder metal-die wall friction.[25-27]

This method was applied to the compaction of solid cylinder and cylindrical rings of copper powder. The predictions show that the relative density distributions are similar to the mean stress distributions, suggesting that powder consolidation is primarily dependent on the mean stress, especially at low compact densities, as shown in Fig. 14 and 15. The trends expected in densification patterns in single-action and double-action compaction were predicted by the simulation, as shown in Fig. 14 and 16. The load-stroke curves indicated slightly higher loads required for single-action press versus double-action press.

Figure 17 shows comparison of pressure distribution of predicted and experimental values[28] in cases of double- and single-action pressing. The authors claim good agreement, but it is not clear what the details of the experiment were, because Fig. 17 does not show a good match of the pressure distributions, especially on the punches. Similar incompatibility of simulated results versus experimental values[29] of relative density distributions are shown in Fig. 18. Whereas these comparisons were performed for simple compression of cylinders and rings, it is difficult to predict the quantitative validity of the model to more complex powder metal compaction processes.

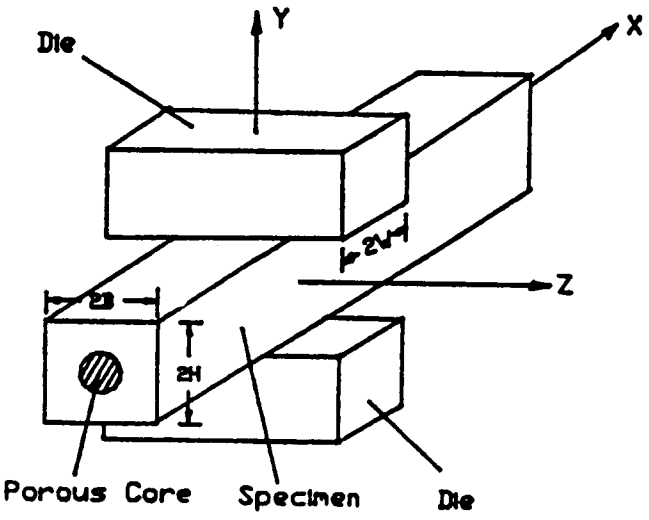

Fig. 22 Flat tool cogging process and specimen.[31]

Ranek *et al.* analyzed the powder forging process for connecting rods.[30] Figure 19 shows the comparisons of bulk densities at various sections of the connecting rod derived by simulation with values derived from powder forged rod. Also, die wall velocities were varied and simulations were performed to determine the effect of die wall velocity on interface friction, as shown in Fig. 20. Figure 21 depicts the relative density gradation in the sections when different die wall velocities were used as fractions of punch velocity at various stages of the deformation simulation. Step 45 denotes the final stage of the process. The results indicate that density variations in the section may be reduced by using a floating die mechanism, thereby imparting some velocity for the die wall (preferably the same as that of the punch).

Void consolidation in forgings made from large ingots have been investigated.[31] Nakajima *et al.*[32] experimented with plasticine specimens to simulate void consolidation. Sun *et al.*[33] and Tanaka *et al.*[34] analyzed the void shrinking condition by the three-dimensional finite element method. However, the artificial defects introduced to study the deformation were too large compared to the dimension of the specimen, and the variation in the geometry of the defects was not considered. Therefore, Sun *et al.*[33] presented a new model for simulation of void consolidation in flat tool forgings. A simplified three-dimensional finite element method was used for modeling the flat tool forging of mild steel specimens with sintered powder metal in their core and for predicting the density change representing the effect on void consolidation. Figure 22 shows the cogging process and the specimen.

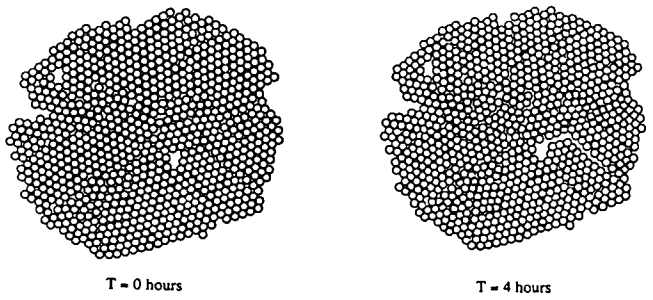

Fig. 23 Packing of glass spheres before (**a**) and after (**b**) 4 hr of sintering. The spheres were 140 mm in diameter and were sintered at 1273 K.[35]

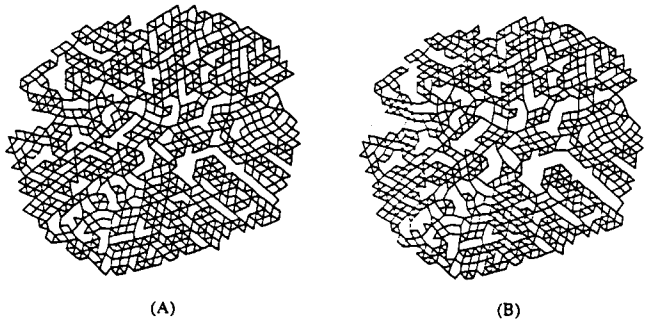

Fig. 24 Truss before and after 4 hr of sintering, $fw = 0.038$.[35]

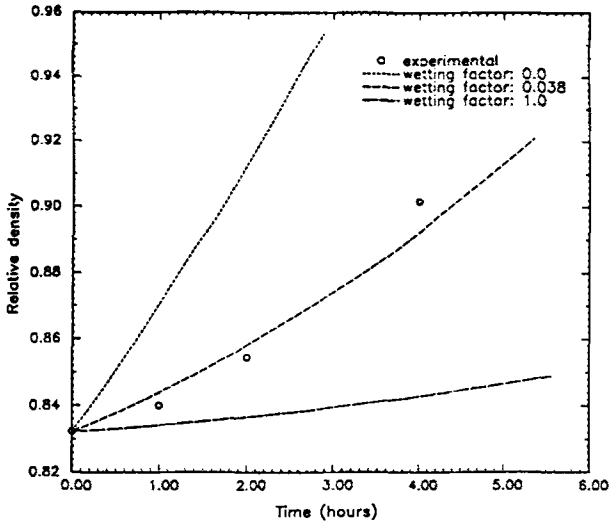

Fig. 25 Relative area density as a function of time.[35]

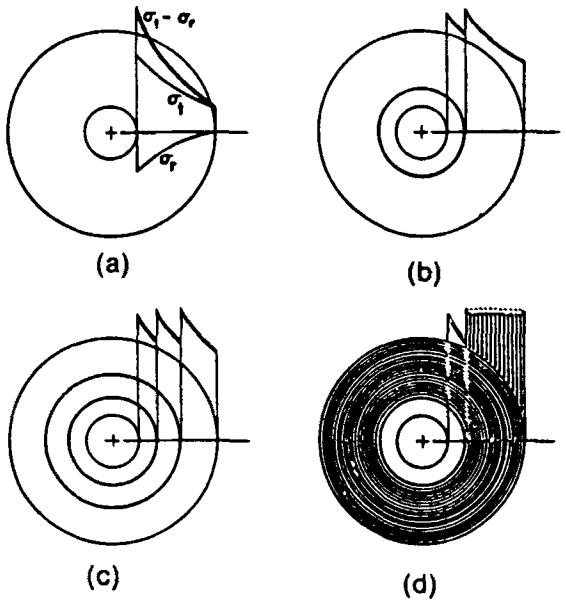

Fig. 26 Axial view of die loading and stresses. (**a**) One-piece die. (**b**) Die insert with one stress ring. (**c**) Die insert with two stress rings. (**d**) Ribbon-wound or wire-wound die insert.[39]

This finite element method approach used a simplified eight-node element and the yield criterion of Doraivelu *et al.*[7] at any material point. The velocity component in the transverse direction of the porous part is limited to reduce errors and for simplification. The results of this method showed good agreement between theory and experiment when bite ratios were greater than 0.7. A criterion E, for the evaluation of void consolidation, was proposed where if γ is positive, a larger value of E implies better consolidation.

The compaction of metal powders has been studied widely under the framework of classical rate-independent plasticity.[35] Sintering phenomenon have been analyzed using numerical methods. Most of the models described for sintering are unit models (two-sphere models, spherical pore models, etc.), which are successful in characterizing only the latter stages of densification where porosity is close to zero. Dawson *et al.*[36] have enhanced these unit models by representing a framework of links, where each link corresponds to an interparticle contact and the nodes correspond to particle centers. The model is based on the principle of virtual work, and the details of the derivation may be found in Ref 33. This model was applied to sintering of a two-dimensional packing of glass spheres (Fig. 23) corresponding to an experiment conducted by Liniger.[38]

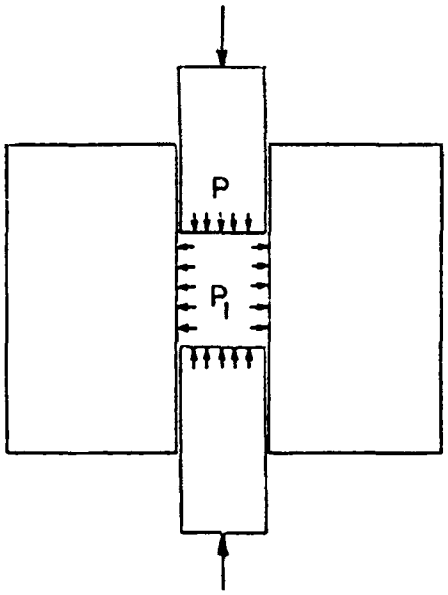

Fig. 27 Schematic view of die loading in powder compaction. Radial pressure P_1 is less than axial compaction pressure P.[39]

In the example considered, the large void grows although the rest of the body shrinks during sintering. Material constants T and h were determined by fitting the results of the unit problem for contact area by sintering, with the experimental values for particles in the packing having only one contact each. The other unknown factor in the experiment was the wetting of the particles to the substrate (graphite). Because initial simulations using the model with no wetting predicted higher sintering rates than observed, viscous friction between the particles and the substrate was introduced by using a wetting factor, fw; if there was no friction $fw = 0$ and if the friction with the substrate was the same as that with a neighboring particle, then $fw = 1$. Figures 24 and 25 show simulation results. It has been shown that the model just described can be applied by varying appropriate parameters to predict observed sintering behavior.

8. Analysis Methods in P/M Forging for Die Design

Application of compaction and repressing to larger parts and harder powders increases the required outer dimensions of

die assemblies and may exceed the die space available in some presses. Therefore, application of shrink rings as shown in Fig. 26 can be used to provide more efficient utilization of material and reduce the die size required for a given pressure and part. A schematic view of die loading in powder compaction is shown in Fig. 27, indicating that the radial pressure P_1 is less than the axial pressure P for porous materials.

Kuhn[39] discussed some techniques for optimum die design based on two-dimensional theory of thick-walled cylinders and derived corrections for actual radial pressure and the constraining effect of unpressurized die sections. Efficient design methods consist of: simultaneously reaching failure at the bore of the die insert and the inside radius of stress ring where stresses are largest. Tungsten carbide inserts and segmented dies should be designed such that the hoop stress is always compressive or zero at the die insert bore, and yielding is imminent at the inside surface of stress ring. The stress ring outside radius should be minimized to reduce the required die space.

Based on above findings, criteria charts and design curves are derived for optimum stress ring dimensions and the required interference fits. In addition, methods for estimation of radial pressure during compaction and for the extra constraint provided by unpressurized die sections above and below the compaction region are discussed for the single stress ring, two stress rings, and ribbon-wound die configurations. Increasing die insert constraint increases the limiting pressure and decreases the outside dimensions of the die assembly. Substantial material savings are possible considering the actual radial pressure P_1, rather than assuming $P_1 = P$. The constraint provided by unstressed material above and below the powder compaction zone has negligible effect on the die design and may be neglected for practical purposes.

Rafanell *et al.*[40] studied the deformations of different shaped dies on compacting of P/M parts using analytical techniques (thick cylinder theories) and photoelastic methods for oblong or square dies with complex stress distributions, using a computer and applying finite element method techniques. For cylindrical dies, the optimum ratio of diameters of the die and shrink ring was approximately 3, and a linear relationship between ring and die outer diameter and the part size was found to exist. The results were more accurate for two-dimensional cases.

9. Conclusions

In the analysis of simple P/M forging processes, slab method analysis can be applied, as shown by Kuhn.[5] Several yield criteria have been proposed for characterizing sintered powder metal behavior and the one most popular appears to be that of Doraivelu *et al.*[7] Sources of other yield criterion were also presented. Friction models for representing friction condition between tool/workpiece were presented including measurement techniques such as the ring test. The concept of forming limit diagrams for analysis of fracture has proved to be practical in upsetting of powder billet.

Numerical methods are applicable also to more complex geometries and forging conditions, notably the work of Kobayashi *et al.*[15,19,20], who developed finite element codes as an extension of the rigid viscoplastic code ALPID by including the compressibility of material. This code has been successful in predicting density distributions and the effects of die wall friction and die velocities during forming operations.[19,20,30] The models developed for compaction show some promise for practical use, although currently predicted results deviate from observed behavior in some cases (for example, Fig. 8). Dawson *et al.*[36] has worked on extending the unit model approach to represent growth of voids by modeling the sintering mechanisms. Future work should perhaps include prediction of the densification during compaction of the green compact besides the densification produced during forming of the compact.

Approaches to die design for P/M tooling have also been presented, primarily by Kuhn.[39] Some of the latest developments in P/M analysis include CAD/CAM approaches to preform and tooling design and the use of expert systems.[8]

Acknowledgments

The authors wish to thank the National Science Foundation sponsored Engineering Research Center for Net Shape Manufacturing, Ohio State University, Dr. Taylan Altan, Director, and Saginaw Division, GM, Dr. Aly Badawy and Mr. Gerry O'Brien, for supporting this review.

References

1. W.H. Huppmann and V. Arnhold, Generations of Metal Products with New Properties by Combined Powder Metallurgy and Deformation Processes, *Advanced Technology of Plasticity,* Vol 11, 943-952.
2. D.C. Drucker and W. Prager, *Quart. Appl. Math., 10,* 157 (1952).
3. N.P. Suh, A Yield Criterion for Plastic, Frictional, Work Hardening Granular Materials, *Int. J. Powder Metall., 5,* 69 (1969).
4. R.J. Green, A Plasticity Theory for Porous Solids, *Int. J. Mechan. Sci., 14,* 215-224 (1972).
5. H.A. Kuhn and C.L. Downey, Jr., Deformation Characteristics and Plasticity Theory of Sintered Powder Materials, *Int. J. Powder Metall., 7,* 15 (1976).
6. S. Shima and M. Oyane, Plasticity Theory for Porous Metals, *Int. J. Powder Metall., 18,* 285 (1976).
7. S.M. Doraivelu, H.L. Gegel, J.S. Gunasekera, J.C. Malas, J.T. Morgan, and J.F. Thomas, Jr. A New Yield Function for Compressible P/M Materials, *Int. J. Mechan., Sci., 26,*(9/10), 527-535 (1984).
8. H.A. Kuhn and B. Lynn Ferguson, *Powder Forging,* Metal Powder Industries Federation, Princeton, NJ (1990).
9. K. Kim, Hot Compaction Equations for Metal Powders and Porous Preforms, *Int. J. Powder Metall., 24,*(1), (1988).
10. H.A. Kuhn and A. Lawley, *Powder Metal Processing—New Techniques and Analyses,* Academic Press, New York, 119-127 (1978).
11. S. Shima and M. Oyane, Plasticity Theory for Porous Metals, *Int. J. Mechan. Sci., 18,* 285 (1976).
12. T. Tabata and S. Masaki, Plane-Strain Extrusion of Porous Materials, *Memoirs of the Osaka Institute of Technology, Series B, 19,*(2) (1975).
13. T. Tabata and M. Oyane, The Slip-Line Field Theory for a Porous Material, *Memoirs of the Osaka Institute of Technology, Series B, 18,*(3), (1975).

14. K. Osakada, J. Nakamo, and K. Mori, Finite Element Method for Rigid-Plastic Analysis of Metal Forming—Formulation for Finite Deformation, *Int. J. Mechan. Sci., 24*, 459 (1982).
15. Y.T. Im and S. Kobayashi, Finite Element Analysis of Plastic Deformation of Porous Materials, in *Metal Forming and Impact Mechanics*, S.R. Reid, Ed., Pergammon Press, Oxford, 103 (1985).
16. R. Hill, *The Mathematical Theory of Plasticity*, Oxford at Clarendon Press (1950).
17. W. Johnson and P.B. Mellor, *Engineering Plasticity*, Nostrand Reinhold, London (1980).
18. S.I. Oh and H.L. Gegel, "ALPIDP—Modeling of P/M Forming by the Finite Element Method," Proc. North American Manufacturing Research Conf., XIV, Minneapolis, SME, 294 (1986).
19. Y.T. Im and S. Kobayashi, Analysis of Axisymmetric Forging of Porous Materials by the Finite Element Method, *Adv. Manufact. Proc., 1*, 473 (1986).
20. Y.T. Im and S. Kobayashi, Coupled Thermo-Viscoplastic Finite Element Analysis of Plane-Strain Compression of Porous Materials, *Adv. Manufact. Proc., 1*, 269 (1980).
21. N. Rebelo and S. Kobayashi, A Coupled Analysis of Viscoplastic Deformation and Heat Transfer—II Applications, *Int. J. Mechan. Sci., 22*, 707 (1980).
22. S.I. Oh, W.T. Wu, J.J. Park, "Application of the Finite Element Method to P/M Forming Processes," Proc. 2nd ICPT, Stuttgart, West Germany, 961 (1987).
23. B.B. Hwang and S. Kobayashi, Deformation Characterization of Powdered Metals in Compaction, *Int. J. Machine Tools Manufact., 30*, 309 (1990).
24. B.B. Hwang and S. Kobayashi, Application of the Finite Element Method to Powdered Metal Compaction Process, *Int. J. Machine Tools Manufact., 31*,(1), 123-137 (1991).
25. J.C. Wang and A.V. Nadkarni, Theoretical Analysis of Powder Compaction and Density Distribution in Long Parts, *Proc. Powder Metall., 37*, 371 (1981).
26. M.E. Shank and J. Wulff, Determination of Boundary Stresses during the Compression of Cylindrical Powder Compacts., *Trans. Am. Inst. Mining Metall. Eng., 185*, 561 (1949).
27. W.A. Nystrom, Copper Base Powder Metallurgy, *New Perspectives in Powder Metallurgy*, vol 7, P.W. Taubenblat, Ed., Metal Powder Industries Federation, Princeton, 142, (1980).
28. R. Davies, High Speed Compaction of Metal Powders Using Petro-Forge Machines, *Powder Metallurgy and Metallurgy and Material Strengthening*, P.R. Dhar, Ed., Chemical Publishing Co., New York, 25 (1970).
29. P. Duwez and L. Zwell, Pressure Distribution in Compacting Metal Powders, *Met. Trans., 185*, 137, Feb (1949).
30. M. Ranek, A. Badawy, and J.J. Park, "Simulation of Densification in Powder Metal Forgings," SAE Tech. Paper No. 890413 (1989).
31. J.X. Sun and Y. Wei, Simulation of Void Consolidation in Flat-Tool Forging, *Advanced Technology of Plasticity*, vol 1 (1990).
32. K. Nakajima *et al.*, Characteristics of Internal Deformation in Hot Free Forging of Heavy Ingots, *J. JSTP, 22*, (246), 697 (1981).
33. J. Sun *et al.*, "Analysis of the Closing and Consolidation of Internal Cavities in Heavy Rotor Forgings by Finite Element Method," Proc. of 2nd ICTP, vol 2, 1057 (1987).
34. M. Tanaka *et al.*, An Analysis of Void Crushing during Flat Die Free Forging, Proc. of 2nd ICTP, vol 2, 1035 (1987).
35. A. Jagota and P.R. Dawson, Unit Problems for the Modeling of Sintering and Traction Induced Compaction of Powders, submitted for publication.
36. P.R. Dawson, A. Jagota, and K.K. Mathur, Applying Micromechanical Models in Deformation Process Simulation," *Interdisciplinary Issues in Materials Processing and Manufacturing*, vol 2, ASME (1987).
37. A. Jagota and P.R. Dawson, A Model for the Sintering and Traction Induced Compaction of Powders, submitted for publication.
38. E.G. Liniger, "Packing and Sintering of Two Dimensional Structures Made from Bimodal Particle Size Distributions," M.S. thesis, Cornell University (1987).
39. H.A. Kuhn, Optimum Die Design for Powder Compaction, *Int. J. Powder Metall. Powder Technol., 14*(4) (1978).
40. J. Rafanell, J. Pares, and C. Molins, Computer Assisted Calculations of Stresses and Deformation in Compacting Dies, *Powder Metall. Int., 15*(3) *(1983)*.